Purification of Multiwalled Carbon Nanotubes by Annealing and Extraction Based on the Difference in van der Waals Potential

Hui Zhang, Cheng H. Sun, Feng Li, Hong X. Li, and Hui M. Cheng*

Shenyang National Laboratory for Materials Science, Institute of Metal Research, Chinese Academy of Sciences, 72 Wenhua Road, Shenyang 110016, China

Received: January 14, 2006; In Final Form: March 10, 2006

The potential energies of van der Waals interactions between two multiwalled carbon nanotubes (MWNTs) as well as two carbon nanoparticles (CNPs) were calculated and compared on the basis of the continuum Lennard-Jones model. The well depth of the potential is 1 order of magnitude higher for MWNTs than for CNPs, indicating that MWNTs and CNPs can be separated from each other through polymer-induced steric stabilization. On the basis of this prediction, a novel method for the purification of MWNTs was proposed. The method involves a high-temperature annealing (2600 °C, 1 h) followed by an extraction treatment with a selected dispersing agent. While the annealing process evaporates the metal particles, the extraction treatment removes CNPs. The quality of the nanotubes obtained after purification was examined by laser Raman, thermogravimetric analysis, and electron microscopy observations.

Introduction

Catalytic thermal chemical vapor deposition (CCVD) synthesis method has been investigated extensively as one of the promising techniques for large-scale production of carbon nanotubes (CNTs).[1−7] The as-synthesized CNTs usually contain structural defects, metal catalysts, and other carbon impurities such as amorphous carbon and carbon nanoparticles (CNPs). However, the purity and structural perfection of CNTs are of great importance to the exploitation of their excellent mechanical and electrical properties for various applications. Therefore, a great deal of effort has been devoted to the development of methods to purify raw CNTs.[8−16] Most of them involve acid treatment and oxidation, which result not only in the elimination of impurities but also in nanotube alteration or even destruction. The high-temperature annealing (graphitization) of CNTs is one of the most efficient methods for the removal of metal particles in the tips or in the hollow core of CNTs[16−19] and also for structural development from disordered fringes to straight, crystalline layers.[20] However, after the annealing, CNPs still exist and become more difficult to remove by normal oxidation method for their graphitization enhancement similar to CNTs. Recently, large fullerenes have been functionalized by alkyl radicals and isolated from raw single-walled carbon nanotube (SWNT) material by extraction in chloroform.[21] But SWNTs would also be expected to experience alkylation under these conditions. Therefore, it is desirable to develop a scalable cleaning method that only removes carbon impurities and metal catalysts without damaging the nanotubes.

It is well-known that filler pigments can be dispersed in a solution via the adsorption of selected dispersing agent in conventional coating production. Such dispersion is considered to be stable as long as the individual pigments do not flocculate, and this approach is well-known as *steric stabilization*. It was recently demonstrated that the steric repulsion among polymer-decorated nanotubes can be employed for the stabilization of SWNT dispersion.[22,23] In particular, the shape and dimensionality of the nanotubes determine the strength, range, and type of intertube van der Waals (vdW) attractions and polymer-induced repulsions.[22b] However, as far as we know, these results focus on SWNTs and the interaction potential between two MWNTs or two CNPs has not been systematically investigated. So there exists an interesting question whether MWNTs can be separated from mixtures of CNPs in the presence of polymer due to their different dimensionalities.

In this study, the potential energies of vdW interactions between two parallel, infinitely long, and perfect MWNTs as well as two CNPs are calculated and compared on the basis of the continuum Lennard-Jones (LJ) model.[24] On the basis of theoretical calculation, we have proposed a purification method involving the high-temperature annealing followed by the dispersant extraction treatment applied to MWNT samples manufactured by CCVD. This novel method is quite effective for the removal of both metal catalyst and CNPs without obvious damage to MWNTs. As a result, high-quality and pure MWNTs are obtained.

Theoretical Calculations

In the calculations, MWNTs are assumed to be infinitely long and perfect; moreover, they are treated as the nesting of a series of concentric SWNTs with a constant interlayer spacing, $c = 3.39$ Å.[25] Hence, the vdW interactions between MWNTs A and B are estimated by summing all potential terms contributed by two single shells,

$$\phi_{AB} = \sum_{i=1}^{n_A}\sum_{j=1}^{n_B}\varphi_{ij} \tag{1}$$

where n_A and n_B are the numbers of layers and φ_{ij} indicates the interaction between two single shells (i and j) and can be evaluated numerically on the basis of the continuum LJ model.[24] LJ parameters for CNTs, σ and ϵ, take the same values from previous works, $\epsilon = 2.39$ meV and $\sigma = 3.415$ Å.[26] Details

* To whom correspondence should be addressed. E-mail: cheng@imr.ac.cn.

10.1021/jp060271h CCC: $33.50
Published on Web 04/25/2006

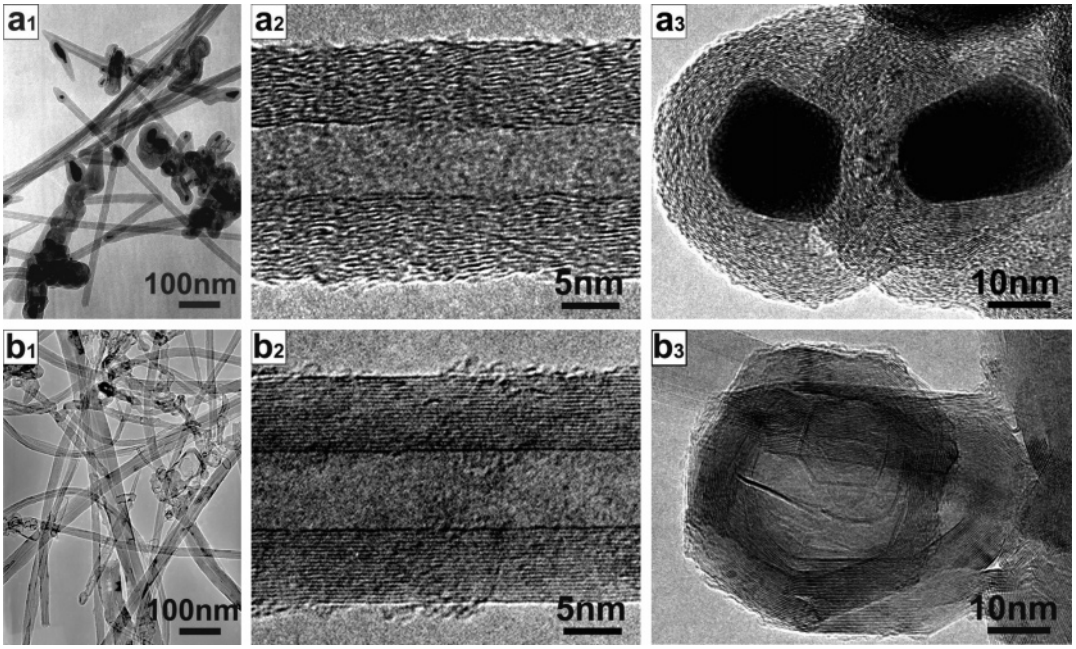

Figure 1. TEM images of the (a) as-synthesized and (b) graphitized MWNT samples.

regarding the calculation of the interaction between two SWNTs can be found elsewhere.[24,29]

The interaction between two CNPs is estimated in a way similar to that indicated by eq 1, and the CNPs are assumed to be multiwalled hollow spheres. However, the integration between two spheres is more difficult than that between two cylindrical surfaces. Generally, the vdW interaction between two buckyballs is usually modeled by the Girifalco potential, which was obtained by integrating a LJ potential for carbon atoms over two spherical shells.[26] An inconvenience for this potential is that only identical shells are involved. To overcome this shortage, a double Yukawa (DY) potential was proposed to fit the carbon−carbon vdW LJ potential and then to integrate on two spheres, which yielded another DY function fitting the Girifalco potential very well.[27] This DY-type potential gives a universal expression for the vdW interaction between two spheres with uniform distributions of carbon atoms,

$$\varphi_{i,j}(r) = \frac{N_i N_j E}{r} \sum_{k=1,2} (-1)^k \frac{\sinh(z_k R_i)}{z_k R_i} \frac{\sinh(z_k R_j)}{z_k R_j} \times \exp[-z_k(r-\sigma)] \quad (2)$$

where r is the distance between the centers of two spheres with radii R_i and R_j, N_i and N_j indicate the numbers of carbon atoms of spheres i and j, respectively; E, z_1, and z_2 are fitted parameters, and σ is the hard core diameter for the LJ potential. LJ parameters for multiwalled CNPs take the values recommended by Girifalco et al., $\epsilon = 2.865$ meV and $\sigma = 3.469$ Å.[26] Details about the DY-type potential can be found elsewhere.[27] So far, the interaction between two multiwalled CNPs can be estimated by summing all terms of φ_{ij}.

Experimental Section

The MWNT samples used in this work were produced by the CCVD method,[4] with micrometer lengths and diameters of 20−50 nm. Thermal annealing of the nanotubes was performed at 2600 °C for 60 min using a graphite-resistance furnace, with a high-purity argon atmosphere. In a typical experiment for the removal of CNPs, dispersing agent 710 (basic urethane copolymer purchased from Tego Chemical Co.) was dissolved in ethanol to form a solution of desired concentration. Graphitized MWNT product was sonicated in the solution for 20 min in a low-power bath (40 W, 60 kHz), which produced a black-colored suspension, along with a precipitate. This suspension was filtered initially by using a sieve (400 mesh). Black filtrate obtained at this stage was collected for observation. The resulting filter cake was again sonicated and washed in ethanol and filtered. The same process was repeated until the final filtrate became clear. The obtained filtered product was dried for further analysis.

The morphology and structure of the samples were studied by scanning electron microscopy (SEM) and transmission electron microscopy (TEM) observations. The Raman measurements were carried out at an excitation wavelength of 632.8 nm. Thermogravimetric analysis (TGA) was carried out under air with a heating rate of 10 °C/min in the temperature range from 30 to 1000 °C.

Results and Discussion

Figure 1a_1 shows the representative TEM image of the as-synthesized MWNT sample, which contains MWNTs with a diameter of 20−50 nm, metal catalyst, and multiwalled CNPs. The main characteristics of these CNTs are their relatively straight morphology and high degree of disorder (undulated fringes) (Figure 1a_2). Dark particles (iron impurities), which originate from the synthesis procedure, not only appeared at the tip of CNTs but also were discontinuously encapsulated in the CNPs (Figure 1a_3). Figure 1b_1 shows the TEM image of the specimen annealed at 2600 °C for 1 h. The most significant effect of the high-temperature treatment is the disappearance of the metal catalyst. However, empty carbon nanopolyhedra still remained in the sample, as shown in Figure 1b_3. This provides the possibility for an efficient separation of carbon nanopolyhedra from CNTs by the extraction assisted with the filtration. In addition, the thermal annealing of CNTs also results in a structural transformation from disordered fringes to straight, crystalline layers (Figure 1b_2).

TGA was used to estimate the purity of CNTs in terms of metal as well as the resistance to oxidation for both pristine

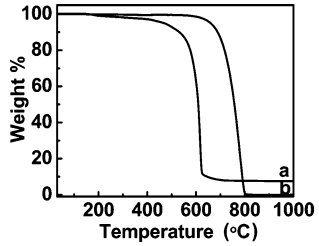

Figure 2. Thermogravimetric analysis of the (a) as-synthesized and (b) graphitized MWNT samples.

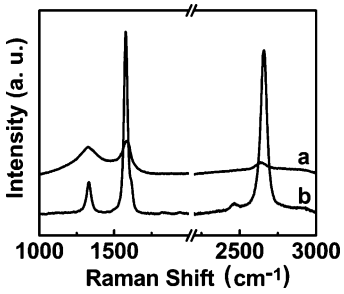

Figure 3. Raman spectra of the (a) as-synthesized and (b) graphitized MWNT samples.

and graphitized CNTs (Figure 2). For the pristine CNTs (Figure 2a), significant weight loss started to occur at 500 °C. The weight loss continued to increase rapidly with temperature, until a stable plateau region appeared at nearly 630 °C. Finally, 92.5% of mass was lost when the experiment was terminated at 1000 °C. This result implies that 5% of the mass of the raw product was iron catalyst. However, for the graphitized CNTs (Figure 2b), weight loss started to occur at 650 °C and a stable plateau region appeared at nearly 800 °C with almost total mass loss at the end of experiment. This result demonstrates that only trace iron existed in the graphitized nanotubes. Thus, the iron impurity in the CNTs could be effectively removed by the high-temperature annealing (T = 2600 °C). It is obvious that graphitized CNTs are oxidized at a significantly higher temperature compared to pristine CNTs; i.e., high-temperature treatment results in the enhanced thermodynamic stability of the treated CNT samples, because the annealing process eliminates the dangling bonds and other structural defects and forms more perfect graphitic structures, as demonstrated by TEM observations.

The above structural change was also confirmed by Raman spectroscopy measurements. Figure 3a displays two characteristic bands of the as-synthesized CNTs. The D-band near 1325 cm^{-1} is related to local defects originating from structural imperfection and amorphous carbon, and the G-band near 1584 cm^{-1} is related to the graphitic E_{2g} symmetry of the interlayer mode, which reflects the structural integrity of the sp^2-hybridized carbon atoms of the nanotubes. The I_D/I_G value of the as-synthesized CNTs is quite high (0.8). However, the high-temperature heat treatment results in a decrease of the I_D/I_G value (0.2), as shown in Figure 3b, which indicates an increase in the crystallite size of graphitic domains. This structural transformation from disordered MWNTs to highly ordered MWNTs, accompanied by the growth of crystallites, is considered to be a stepwise process: (1) straightening and rearrangement of distorted small graphene layers; (2) fusion between graphene layers; (3) growth to larger graphene layers along the tube axis and then removal of stacking faults between graphene layers within a confined space.[20] Therefore, the high-temperature annealing is an effective method of removing both the catalyst particles and the microstructural defects within the nanotubes.

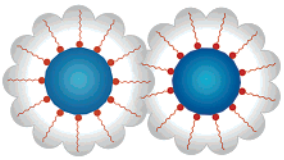

• anchor group ~~~ polymer chain ○ boundary of steric stabilization

Figure 4. Sketch of a particle stabilized by polymer molecules (not to scale).

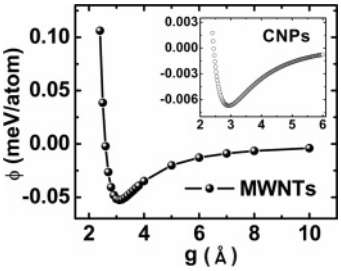

Figure 5. Potential energy per atom for MWNTs and CNPs.

Besides metal catalyst, various types of CNPs are present in the as-synthesized samples such as Fe-filled carbon nanocapsules, onion-like carbon, and carbon lamellas. After the Fe-filled carbon nanocapsules are turned into hollow nanopolyhedra by high-temperature annealing, significant amounts of nanopolyhedra and lamellar carbon are found in the graphitized MWNT samples. Thus, the following purification process focuses on the separation of CNPs from MWNTs.

Commercially available dispersing agents for carbon black have a two-component structure: one is specific anchoring groups which can be strongly adsorbed on the particle surface; the other is polymeric chains which dangle into the solvent and repel other polymers. In the coating production, a pigment is often sterically stabilized when its surface is completely covered by polymers, since strong interactions between polymers and solvent prevent the polymers from being too close and contacting with each other (Figure 4). *Steric stabilization* relies on the adsorption of a layer of polymer chains on the surface of the pigment. The thickness of the anchored polymer layer (h) scales with the polymer chain length (N) and its surface coverage (σ), which can be expressed as $h \propto N\sigma^{1/3}$.[28] The linear increase of the thickness with the molecular weight serves as an important tool in the manipulation of the range of the interactions. In addition, stability of the dispersion is affected by the size, shape, and dimensionality of the dispersed objects.[22b] Considering that CNPs and MWNTs present different dimensionalities, is it possible to separate them on the basis of their dimensionality-dependent differences in vdW interparticle potentials? The following calculation results gave a positive answer.

The potential energies per atom for MWNT−MWNT and CNP−CNP are shown in Figure 5 and its inset, respectively. The horizontal axis in Figure 5 labels the distance between the sidewalls, rather than the centers, of two interacting entities. To compare with each other, the outer diameters of MWNTs and CNPs employed in Figure 5 are close, 40.0 nm for MWNT and 39.7 nm for CNP. Three important findings are immediately evident. The first is that the well depth of the potential is 1 order of magnitude higher for MWNTs than for CNPs (0.0525 meV/atom for MWNTs vs 0.0067 meV/atom for CNPs). At the equilibrium distance, the potential energy per atom is 5.87 meV/atom for (10, 10)−(10, 10) SWNT and 4.63 meV/atom for C_{60}−C_{60}.[29] On the basis of the above results, the interaction per atom between CNP and MWNT is supposed to be smaller than MWNT−MWNT and larger than CNP−CNP. The second is

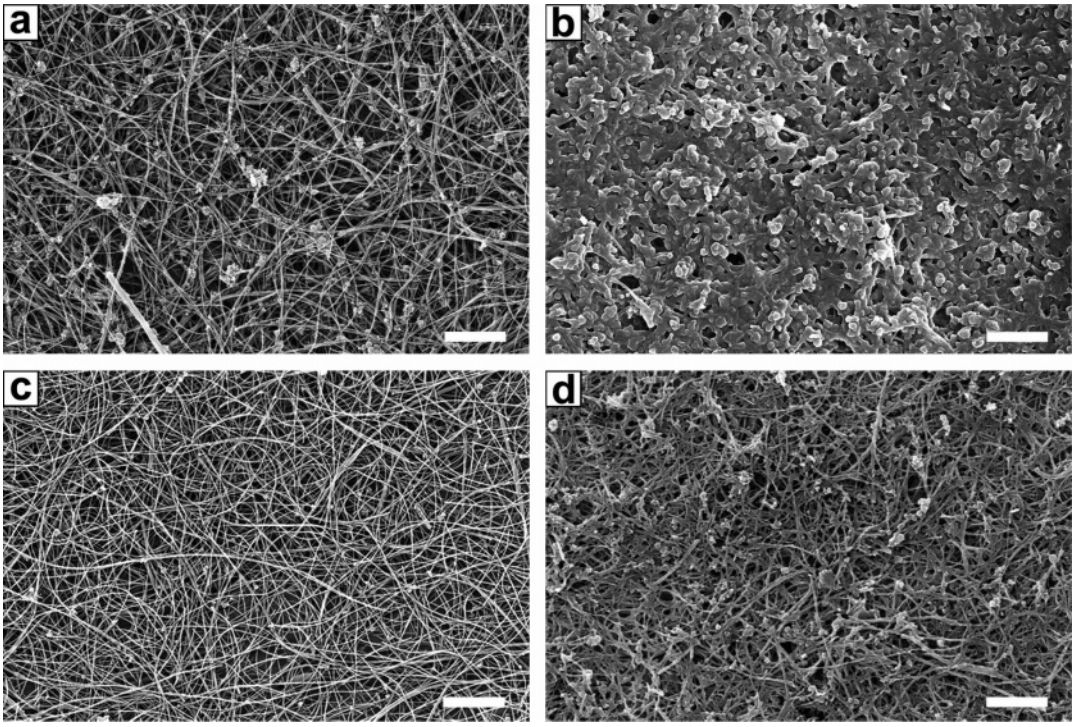

Figure 6. SEM micrographs of (a) the graphitized MWNTs, (b) the dried filtrate phase, and (c) the final filtered product obtained after extraction with a solution of 0.08 wt % polymer, and (d) the dried filtrate phase obtained after extraction with a solution of 0.2 wt % polymer (scale bar is 2 μm).

that the equilibrium distance g_0 between two MWNTs (g_0 = 3.12 Å) is close to that of CNPs (g_0 = 2.94 Å). The values of g_0 for MWNT−MWNT and for CNP−CNP are close to those of their respective single shells, g_0 = 2.96 and 3.15 Å for C_{60}−C_{60} and (10, 10)−(10, 10).[29] In fact, g_0 is almost independent of the numbers of layers of MWNTs and CNPs. The third is that, even when the distance g between the sidewalls of two MWNTs is up to 10 Å, the potential energy per atom (0.0040 meV/atom) is still close to the well depth for CNP−CNP (0.0067 meV/atom). Moreover, in the range of $g > g_0$, the interaction is dominated by the attractive force which decreases slightly. On the basis of the above simple estimations, two points can be deduced: (1) MWNTs are more apt to aggregate together than CNPs; (2) due to the remarkable difference of the vdW interactions for MWNT−MWNT and CNP−CNP, the polymer chain length and surface coverage necessary for inducing steric repulsion in CNP dispersion are much lower than those required for dispersion of MWNTs. This effect suggests that a proper choice of polymer may result in the separation of CNPs from MWNTs.

On the basis of the above theoretical calculation of the potential energies of vdW interactions between two parallel, infinitely long, and perfect MWNTs as well as two CNPs, the following experiment was designed. A graphitized sample containing MWNTs along with CNP impurities was sonicated in the ethanol solution of the dispersing agent 710 at concentrations between 0.04 and 0.3 wt %. The resultant black suspension was filtered using a sieve (400 mesh) and washed with ethanol. Both the filtrate and the final filter cake were imaged by SEM. As shown in Figure 6a, the raw graphitized MWNT sample is characterized by the presence of long and densely entangled nanotubes together with a significant amount of CNPs aggregating as clusters due to the vdW interactions. After the graphitized MWNT sample was dispersed in an ethanol solution of 0.08 wt % polymer, the dried filtrate phase (Figure 6b) is obviously enriched by nontube structures which were coated by a dense layer of polymer, suggesting that CNPs were preferable to be sterically stabilized in the solution phase in the presence of polymer and thus they can be separated from MWNTs by subsequent filtration. When the concentration of the dispersing agent 710 is in the range of 0.04−0.1 wt %, *only* CNPs suspend while CNTs deposit at the bottom. Figure 6c shows an image of the final filter cake, with a minute quantity of CNPs. Thus, high-quality and pure MWNTs are obtained. The yield of CNTs is about 90%. The mass loss of 10% mainly includes the evaporated metal impurity during the annealing process and CNPs by the extraction. These observations are consistent with theoretical calculation results: the well depth of the potential is 0.0067 meV/atom for CNPs, which is much smaller than for MWNTs (0.0525 meV/atom), indicating that CNPs can be effectively removed from MWNTs in the presence of polymer solution at a certain concentration since the polymer-induced repulsion only effectively prevents the aggregation of individual CNPs. According to the above calculation results, to separate MWNTs from each other and form a stable dispersion, a higher grafting density is required. With increasing the polymer concentration, MWNTs can also be stabilized in the solution phase as well as CNPs (Figure 6d) since their surfaces were covered by enough polymers. Therefore, the observed selectivity is an important consequence of the dependence of the vdW potential on their dimensionalities and offers a generic approach to the separation of MWNTs from a mixture of CNPs.

Conclusions

MWNT samples prepared by CCVD method are usually accompanied by structural defects, metal catalyst, and CNPs. Graphitization is an effective procedure for removing microstructural defects as well as metal particles in the nanotubes. The interaction potential between two parallel, infinitely long, and perfect MWNTs as well as two CNPs has been calculated and compared on the basis of the continuum LJ model. It was found that the attractive potential between two CNPs is relatively

low and in a short range. Therefore, the polymer chain length and surface coverage for the dispersion of CNPs is lower than that needed for the dispersion of MWNTs. On the basis of this theoretical prediction, CNPs and MWNTs are effectively separated from each other by choosing an appropriate polymer and suitable concentration (for instance, 0.04−0.1 wt % for the dispersing agent 710), and an effective and nondestructive method for the purification of MWNT is developed.

Acknowledgment. This work was supported by the National Natural Science Foundation of China (Grant 50328204) and the Hi-Tech Research and Development program of China (Grant 2002AA327110).

References and Notes

(1) Dal, H. J.; Rinzler, A. G.; Nikolaev, P.; Thess, A.; Colbert, D. T.; Smalley, R. E. *Chem. Phys. Lett.* **1996**, *260*, 471.

(2) Terrones, M.; Grobert, N.; Olivares, J.; Zhang, J. P.; Terrones, H.; Kordatos, K.; Hsu, W. K.; Hare, J. P.; Townsend, P. D.; Prassides, K.; Cheetham, A. K.; Kroto, H. W.; Walton, D. R. M. *Nature* **1997**, *388*, 52.

(3) Rao, C. N. R.; Sen, R.; Satishkumar, B. C.; Govindaraj, A. *Chem. Commun.* **1998**, 1525.

(4) Fan, Y. Y.; Li, F.; Cheng, H. M.; Su, G.; Yu, Y. D.; Shen, Z. H. *J. Mater. Res.* **1998**, *13*, 2342.

(5) Andrews, R.; Jacques, D.; Rao, A. M.; Derbyshire, F.; Qian, D.; Fan, X.; Dickey, E. C.; Chen, J. *Chem. Phys. Lett.* **1999**, *303*, 467.

(6) Kamalakaran, R.; Terrones, M.; Seeger, T.; Kohler-Redlich, P.; Ruhle, M.; Kim, Y. A.; Hayashi, T.; Endo, M. *Appl. Phys. Lett.* **2000**, *77*, 3385.

(7) Endo, M.; Kim, Y. A.; Fukai, Y.; Hayashi, T.; Terrones, M.; Terrones, H.; Dresselhaus, M. S. *Appl. Phys. Lett.* **2001**, *79*, 1531.

(8) Dujardin, E.; Ebbesen, T. W.; Krishnan, A.; Treacy, M. M. J. *Adv. Mater.* **1998**, *10*, 611.

(9) Chiang, I. W.; Brinson, B. E.; Huang, A. Y.; Willis, P. A.; Bronikowski, M. J.; Margrave, J. L.; Smalley, R. E.; Hauge, R. H. *J. Phys. Chem. B* **2001**, *105*, 8297.

(10) Park, Y. S.; Choi, Y. C.; Kim, K. S.; Chung, D. C.; Bae, D. J.; An, K. H.; Lim, S. C.; Zhu, X. Y.; Lee, Y. H. *Carbon* **2001**, *39*, 655.

(11) Hou, P. X.; Bai, S.; Yang, Q. H.; Liu, C.; Cheng, H. M. *Carbon* **2002**, *40*, 81.

(12) Chiang, I. W.; Brinson, B. E.; Smalley, R. E.; Margrave, J. L.; Hauge, R. H. *J. Phys. Chem. B* **2001**, *105*, 1157.

(13) Chen, X. H.; Chen, C. S.; Chen, Q.; Cheng, F. Q.; Zhang, G.; Chen, Z. Z. *Mater. Lett.* **2002**, *57*, 734.

(14) Li, F.; Cheng, H. M.; Xing, Y. T.; Tan, P. H.; Su, G. *Carbon* **2000**, *38*, 2041.

(15) Strong, K. L.; Anderson, D. P.; Lafdi, K.; Kuhn, J. N. *Carbon* **2003**, *41*, 1477.

(16) Wang, Y.; Wu, J.; Wei, F. *Carbon* **2003**, *41*, 2939.

(17) Andrews, R.; Jacques, D.; Qian, D.; Dickey, E. C. *Carbon* **2001**, *39*, 1681.

(18) Huang, W.; Wang, Y.; Luo, G. H.; Wei, F. *Carbon* **2003**, *41*, 2585.

(19) Endo, M.; Nishimura, K.; Kim, Y. A.; Hakamada, K.; Matushita, T.; Dresselhaus, M. S.; Dresselhaus, G. *J. Mater. Res.* **1999**, *14*, 4474.

(20) Kim, Y. A.; Hayashi, T.; Osawa, K.; Dresselhaus, M. S.; Endo, M. *Chem. Phys. Lett.* **2003**, *380*, 319.

(21) Sadana, A. K.; Liang, F.; Brinson, B.; Arepalli, S.; Farhat, S.; Hauge, R. H.; Smalley, R. E.; Billups, W. E. *J. Phys. Chem. B* **2005**, *109*, 4416.

(22) (a) Bandyopadhyaya, R.; Nativ-Roth, E.; Regev, O.; Yerushalmi-Rozen, R. *Nano Lett.* **2002**, *2*, 25. (b) Shvartzman-Cohen, R.; Nativ-Roth, E.; Baskaran, E.; Levi-Kalisman, Y.; Szleifer, I.; Yerushalmi-Rozen, R. *J. Am. Chem. Soc.* **2004**, *126*, 14850.

(23) Shvartzman-Cohen, R.; Levi-Kalisman, Y.; Nativ-Roth, E.; Yerushalmi-Rozen, R. *Langmuir* **2004**, *20*, 6085.

(24) Sun, C. H.; Yin, L. C.; Li, F.; Lu, G. Q.; Cheng, H. M. *Chem. Phys. Lett.* **2005**, *403*, 343.

(25) Charlier, J. C.; Michenaud, J. P. *Phys. Rev. Lett.* **1993**, *70*, 1858.

(26) Girifalco, L. A. *J. Phys. Chem.* **1992**, *96*, 858.

(27) Guerin, H. *J. Phys.: Condens. Matter* **1998**, *10*, L527.

(28) Milner, S. T. *Science* **1991**, *251*, 905.

(29) Girifalco, L. A.; Hodak, M.; Lee, R. S. *Phys. Rev. B* **2000**, *62*, 13104.